

# Modeling of pile end resistance considering the area of influence around the pile tip

Junichi Hyodo<sup>\*1</sup>, Yoshio Shiozaki<sup>2</sup>, Yukio Tamari<sup>3a</sup>, Osamu Ozutsumi<sup>4a</sup> and Koji Ichii<sup>5a</sup>

<sup>1</sup>Civil Engineering Division, Tokyo Electric Power Services Co. Ltd, Japan, 7-12 Shinonome 1-chome Koto-ku, Tokyo 135-0062, Japan

<sup>2</sup>Steel Research Laboratory, JFE Steel Corporation, Japan

<sup>3</sup>Business Incubation Unit, Tokyo Electric Power Services Co. Ltd, Japan

<sup>4</sup>Meisoshu Corporation, Japan

<sup>5</sup>Faculty of Societal Safety Sciences, Kansai University, Japan

(Received September 25, 2018, Revised February 10, 2019, Accepted February 12, 2019)

**Abstract.** The finite element method (FEM) is widely used to evaluate the seismic performance of pile-supported buildings. However, there are problems associated with modeling the pile end resistance using the FEM, such as the dependence on the mesh size. This paper proposes a new method of modeling around the pile tip to avoid the mesh size effect in two-dimensional (2D) analyses. Specifically, we consider the area of influence around the pile tip as an artificial constraint on the behavior of the soil. We explain the problems with existing methods of modeling the pile tip. We then conduct a three-dimensional (3D) analysis of a pile in various soil conditions to evaluate the area of influence of the soil around the pile tip. The analysis results show that the normalized area of influence extends approximately 2.5 times the diameter of the pile below the pile tip. Finally, we propose a new method for modeling pile foundations with artificial constraints on the nodal points within the area of influence. The proposed model is expected to be useful in the practical seismic design of pile-supported buildings via a 2D analysis.

**Keywords:** area of influence; 2D analysis; pile-supported building

## 1. Introduction

The finite element method (FEM) is widely used to evaluate the seismic performance of various facilities in Japan, such as buildings with pile foundations and sheet pile quay walls (Architectural Institute of Japan 2001, The Overseas Coastal Area Development Institute of Japan 2009). In dynamic analyses, the piles of a structure must be appropriately modeled to properly consider the pile-soil interaction.

In the FEM modeling of pile-supported buildings, the following three components of pile resistance must be considered: the lateral capacity, shaft friction, and pile end resistance. For the lateral capacity, modeling on the pile-soil interaction has been proposed (Hussien *et al.* 2010, Fatahi *et al.* 2014, Tamari *et al.* 2018), whereas a nonlinear spring element is typically used for the shaft friction (Architectural Institute of Japan 2001). The observation of the shaft friction has been conducted either (Barr *et al.* 2013). However, modeling the pile tip is difficult.

Currently, a simple modeling approach is employed for the pile tip, as the pile tip element shares a node with the adjacent ground elements. However, this can result in various problems including the mesh size effect and strain localization.

Many studies have been conducted on the end-bearing

capacity of piles (Terzaghi 1943, Meyerhof 1951, Berezantsev *et al.* 1961, Vesic 1972, Hirayama 1988, Yasufuku *et al.* 2001, Manandhar *et al.* 2012, 2013, Kumara *et al.* 2015). To consider nonlinear response developed at the pile end, many types of models has been proposed (i.e., Wang *et al.* 2012, Zhang *et al.* 2012). Hirayama (1990), Zhang *et al.* (2014) and Zhang *et al.* (2016) showed that the pile end resistance and the pile tip displacement have a hyperbolic correlation.

Yasufuku and Hyde (1995) subsequently proposed a model describing the end-bearing capacity of a pile based on the spherical cavity expansion theory. Based on the same theory, Yang (2006) obtained the area of influence for the pile end resistance. These findings should be incorporated when developing an appropriate means of modeling the pile tip in two-dimensional (2D) analyses.

In this paper, we propose a new pile tip modeling method wherein the influence area for the pile end resistance is considered while avoiding the mesh size effect. The rest of this paper is organized as follows. First, the influence area of the soil around the pile tip is examined by performing a sophisticated three-dimensional (3D) analysis in Chapter 3. A 2D analysis of a pile foundation is then conducted to demonstrate the effectiveness of the proposed method in Chapter 4.

## 2. Modeling of the pile tip in 2D analyses

### 2.1 Target pile tip behaviour

Hirayama (1990) demonstrated that the pile end

\*Corresponding author, Engineer

E-mail: [hyoudou@tepsco.co.jp](mailto:hyoudou@tepsco.co.jp)

<sup>a</sup>Ph.D.

resistance and the pile tip displacement have a hyperbolic correlation, as shown in Fig. 1 and expressed in Eq. (1). It was further reported that the concept of hyperbolic correlation is consistent with the results of in situ tests. As there are only two parameters in the hyperbolic correlation, it is suitable for practical use. Therefore, we employed the hyperbolic correlation in this study for the nonlinear spring element between the pile tip and the ground.

$$q = \frac{z_e}{a_e + b_e z_e} \quad (1)$$

$$a_e = \frac{z_{ref,e}}{q_{ult}} = \frac{0.25}{q_{ult}} \quad b_e = \frac{1}{q_{ult}} \quad (2)$$

where the reference displacement  $z_{ref,e}$  ( $= 0.25D_e$  (m)) is for sandy soil,  $D_e$  is the pile diameter, and  $q_{ult}$  is the ultimate value of the pile end resistance. Hirayama (1990) verified the applicability of Eq. (2) by using the results of the loading tests (BCP Committee (1971)). Also, we can modify the reference displacement  $z_{ref,e}$  in Eq. (2) based on the back analysis of the loading tests. However, as it is difficult to calculate the maximum value of the pile end resistance  $q_{ult}$ , the Japanese design code (e.g., Architectural Institute of Japan 2001) defines the end-bearing capacity of a pile as the pile end resistance at  $0.1D_e$ .

Substituting  $z_e = 0.1D_e$  (m) in Eq. (1) for the pile tip settlement, it can be rewritten as follows.

$$q_{0.1} = \frac{0.1D_e}{a_e + b_e \cdot 0.1D_e} \quad (3)$$

The following equation is obtained by combining Eqs. (2) and (3).

$$q_{0.1} = 0.286q_{ult} \quad (4)$$

From Eqs. (2) and (4), the following equations can be obtained for parameters  $a_e$  and  $b_e$

$$a_e = \frac{0.0715D_e}{q_{0.1}} \quad b_e = \frac{0.286}{q_{0.1}} \quad (5)$$

As a result, we can determine the load-settlement relationship from the pile diameter ( $D_e$ ) and the pile end resistance for a settlement of  $0.1D_e$ . Note that the target pile tip behavior is assumed to follow a hyperbolic relationship.

## 2.2 Existing pile tip models (Models A and B)

Fig. 2(a) shows the simplest 2D analysis pile foundation model (Model A) in current use. This model can be used to express the lateral capacity and shaft friction via pile-soil interaction elements and nonlinear spring elements. For the pile end resistance, this model assigns the same displacement to the node of the pile tip and the node of the corresponding ground. However, this approach causes various problems at the pile tip, including stress concentration, which will be explained in section 2.3.

Fig. 2(b) shows the most advanced current 2D analysis pile foundation model (Model B), which is a revised version of Model A. Here, the pile end resistance is modeled using a

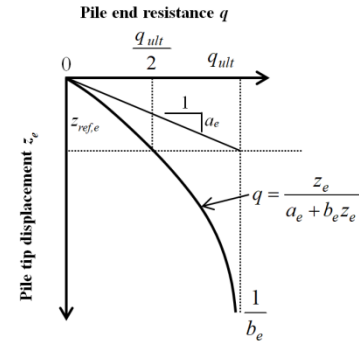


Fig. 1 Relationship between the pile end resistance and the pile tip displacement (Hirayama 1990)

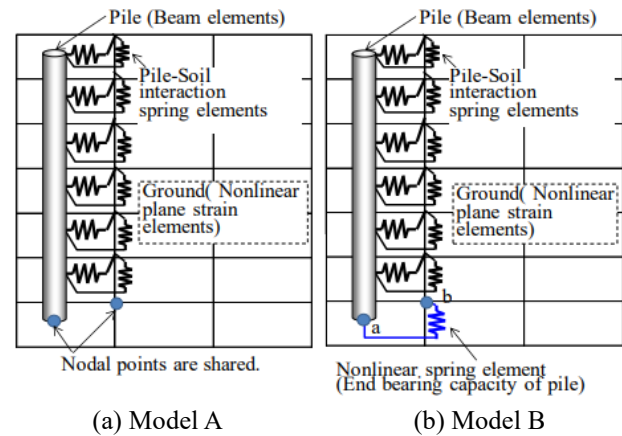


Fig. 2 Models of pile-soil interaction in 2D analysis

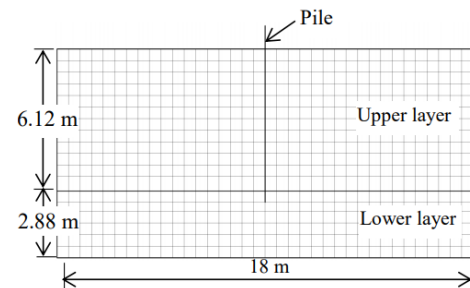


Fig. 3 2D mesh model used in the analysis

Table 1 Soil parameters

Characteristics	Upper layer	Lower layer
Relative density $D_r$ (%)	60	90
Wet density $\rho$ ( $t/m^3$ )	1.93	1.99
Shear modulus $G_{ma}$ (kPa) *1	$8.97 \times 10^4$	$1.51 \times 10^5$
Bulk modulus $K_{ma}$ (kPa) *1	$2.34 \times 10^5$	$3.94 \times 10^5$
Reference confining effective stress $\sigma'_{ma}$ (kPa) *1	98.0	98.0
Reference parameter $m_G, m_K$ *2	0.5	0.5
Internal friction angle $\phi$ (°)	39.86	42.05

\*1  $G_{ma}$  and  $K_{ma}$  are shear modulus and bulk modulus at a reference confining effective stress  $\sigma'_{ma}$

\*2 Shear modulus  $G$  and bulk modulus  $K$  for arbitrary mean effective confining stress  $\sigma'_m$  are calculated by the following equations.

$$G = G_{ma} (\sigma'_m / \sigma'_{ma})^{m_G}, \quad K = K_{ma} (\sigma'_m / \sigma'_{ma})^{m_K}$$

nonlinear hyperbolic spring element placed in series between the pile tip and the ground. In addition, in this model, the ground nodal point of the pile tip spring element can be moved. However, as explained in Section 2.3, some problems remain with the use of this model.

### 2.3 Performance of existing pile tip models

In practice, many designs are based on the results of 2D analysis. Therefore, we conducted several analyses to examine the applicability of the various models at the pile tip using the 2D analysis program in the FLIP series (Iai *et al.* 1992). Fig. 3 shows the 2D mesh used in the analysis. In the analysis, the ground is made of two layers, namely the upper and lower, and the relative density of the upper layer is 60% and that of the lower layer is 90%. Tables 1 and 2 list the soil and pile parameters, respectively. Fully drained conditions were assumed. Two-dimensional multi-spring elements (Towhata and Ishihara 1985) were used for the soil, and the pile was modeled using linear beam elements.

The lateral boundaries in the horizontal direction were fixed; the bottom boundary was fixed; and the pile end resistance was modeled using the nonlinear spring elements proposed by Hirayama (1990). Table 3 lists the parameters of these elements.

The pile penetration was represented as an enforced displacement at the pile head nodes. The load-settlement relationships in the following analysis were obtained via a 2D analysis conducted with the above parameters.

Fig. 4(a) shows the effect of the mesh size on Model A. The target is the load-settlement relationship of the nonlinear spring element at the pile tip. For mesh sizes of 0.1, 0.25, 0.5, and 0.8 m, the analysis results are inconsistent with the target. For mesh sizes of 0.5 and 0.8 m, the pile end resistance is overestimated. However, for mesh sizes of 0.1 and 0.25, the pile end resistance is underestimated, because of the high stress for a small mesh size element at the pile tip. Thus, in the case of fine meshes, strain localization in the ground elements around pile tip was occurred. As a result, Model A is unstable, as the pile end resistance is found to depend on the mesh size.

As the previous study of mesh size effect, Kobayashi (1988) reported that bearing capacity in a smaller mesh size by using FEM were smaller. Also, Wakai (1995) reported that bearing capacity for horizontal direction in a smaller mesh size was smaller. Our results are consistent with these studies. Fig. 4(b) shows the analysis results of the effect of the mesh size on Model B. Here, the target is the same as that used in the analysis of Model A. In this case, the analysis results with fine meshes are underestimated, because the ground deformation at the pile tip was counted twice : movement of nonlinear spring element (virtual distance between point a and point b in Fig. 2(b)) and movement of the nodal point (point b in Fig. 2(b)) in the ground. Here, the pile tip displacement of nonlinear spring defined in Fig. 1 is the movement of point a in Fig. 2(b) assuming the point b is fixed. Thus, if point b is not fixed, the settlement of the pile is overestimated as much as the point b moves.

In general, the error in an FEM analysis can be reduced by using a smaller mesh size. Accordingly, the analysis with

Table 2 Pile parameters

Characteristics	
Diameter (m)	0.48
Thickness (m)	0.032
Young's modulus (kPa)	$1.05 \times 10^9$
Poisson's ratio	0.35
Area (m <sup>2</sup> )	0.045

Table 3 Parameters of the nonlinear spring element

Characteristics	
$q_{0.1}$ (kN/m <sup>2</sup> )	2625
$a_e$ (m/(kN/m <sup>2</sup> ))	$1.31 \times 10^{-5}$
$b_e$ (1/(kN/m <sup>2</sup> ))	$1.09 \times 10^{-4}$
$q_{ult}$ (kN/m <sup>2</sup> )	9178
Area $A$ (m <sup>2</sup> )	0.181
$q_{ult} A$ (kN)	1661

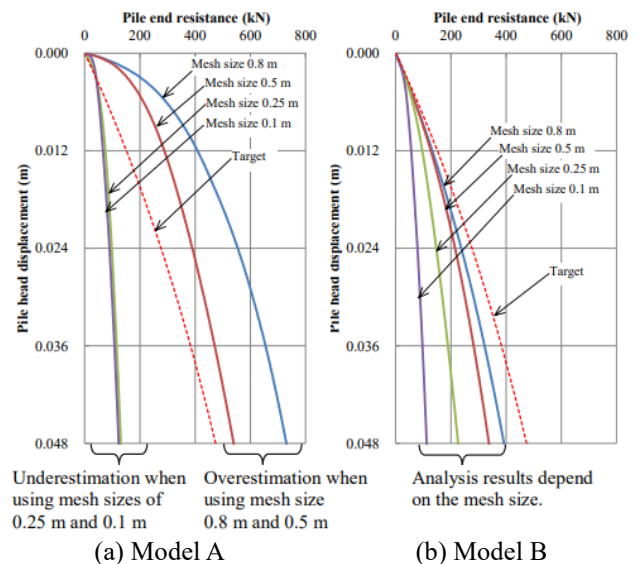


Fig. 4 Relationship between the pile end resistance and the pile head displacement

a small mesh should agree with the target. However, in this case, it was found that a larger mesh size (of 0.8 m) was required for the results to agree with the target. Above a certain level, the mesh size reduces the effect of the stress concentration, thereby constraining the deformation of the mesh. Accordingly, the double counting of the settlement can be avoided.

### 2.4 Proposal model (Model C)

As discussed above, there are problems with the use of both Models A and B. However, Model B, in which a nonlinear spring element connects the pile tip ground in series, is the most advanced model currently in use for simulating pile settlements. However, this model has a problem in that the ground deformation is counted twice. To avoid this problem, we propose a new model, namely

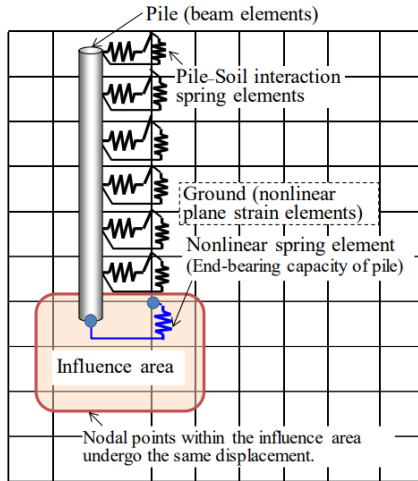


Fig. 5 Proposed Model C

Table 4 Comparison of different pile-soil interaction models

	Model A	Model B	New model C
Concept	Pile and soil at the pile tip have the same displacement.	Pile end resistance is modeled using nonlinear spring elements.	Pile end resistance is modeled using nonlinear spring elements. The ground nodal points within the influence area are constrained.
Pile end resistance	Pile end resistance does not agree with the target.	Pile end resistance agrees with the target if the mesh is large enough.	Pile end resistance agrees well with the target.
Features	Simple	Possible overestimation of the settlement	Difficulty in assessing the influence area

Table 5 Soil parameters

Characteristics	Lower layer Case 1	Lower layer Case 2	Lower layer Case 3
Relative density $D_r$ (%)	45	60	90
Wet density $\rho$ ( $t/m^3$ )	1.99	1.99	1.99
Shear modulus $G_{ma}$ (kPa)	$6.33 \times 10^4$	$8.97 \times 10^4$	$1.51 \times 10^5$
Bulk modulus $K_{ma}$ (kPa)	$1.65 \times 10^5$	$2.34 \times 10^5$	$3.94 \times 10^5$
Reference confining effective stress $\sigma'_{ma}$ (kPa)	98.0	98.0	98.0
Reference parameter $m_G, m_K$	0.5	0.5	0.5
Cohesion $C$ (kPa)	0.0	0.0	0.0
Internal friction angle $\phi$ ( $^\circ$ )	30, 35, 40, and 45	30, 35, 40, and 45	30, 35, 40, and 45

Model C, in which some of the ground nodal points within the area of influence for the end-bearing capacity of a pile are constrained to undergo the same deformation. Fig. 5 shows the details of the proposed Model C. Table 4 gives a comparison of the characteristics of the three pile-soil interaction models. Also, we can consider the influence of shaft friction (Hyodo *et al.* 2017). However, for the simplicity, shaft friction is ignored in this study.

The proposed model is more advantageous, as the mesh size effect and settlement overestimation can be avoided. However, this model requires the area of influence to be appropriately selected.

### 3. Evaluation of the area of influence around the pile tip

#### 3.1 3D analysis of the pile end resistance

We conducted a 3D analysis to examine the area of influence for the end-bearing capacity of a pile. The 3D analysis was performed using an analysis model (12 m high, 18 m long, and 6 m wide). A quarter (1/4) of the target model, shown in Fig. 6, was analyzed to save computational time. The pile penetration was represented as an enforced displacement at the pile head, and the x, y, and z axes represent the length, width, and vertical axis, respectively. The model comprises two layers of saturated sand (upper layer  $D_r = 60\%$ ; lower layer  $D_r = 45, 60, \text{ and } 90\%$ ). The analysis was conducted using the 3D analysis program in the FLIP ROSE series, i.e., FLIP (3D version) Ver 1.6.2 (Iai 1993), assuming fully drained conditions. Table 5 lists the soil parameters. The pile parameters are the same as those listed in Table 2. In addition, 3D multi-spring model elements with the Mohr-Coulomb failure criteria was employed for the soil.

In this analysis, the stress-strain relationship in each arbitrary shear direction was modeled as a hyperbolic relationship (Towhata and Ishihara 1985), and shell elements were used for the pile, with joint elements inserted between the soil and the pile. The nodes at the pile tip and the ground, which is in contact with the pile tip, were combined to obtain the same movement in the z-direction. Roller boundary conditions were applied to the side boundaries (xz-plane and yz-plane), whereas the bottom boundary was fixed. On the symmetrical plane ( $y = 0$ ), the movement in the y-direction and rotational movement about the x and z axes were fixed. To focus on the end-bearing capacity of the pile, the pile-soil friction along the pile was ignored. Consequently, the bearing capacity at the pile head and that at the pile tip were the same.

#### 3.2 Shear strain around pile tip

Fig. 7 shows the relationship between the pile end resistance and the pile head displacement in Case 3 (lower layer  $D_r = 90\%$ ). The figure also shows that the pile end resistance increases with the increase in the internal friction angle.

Fig. 8 shows the distribution of the maximum shear strain in Case 3 (Lower layer  $D_r=90\%$ ) when the settlements are 1, 5, and 10% of the pile diameter. The shape of the pressure bulb is considered a region of high vertical stress and large strain. In this case, the area associated with the high stress and strain was approximately two to three times the pile diameter in both the vertical and horizontal directions. In this study, we defined the influence area for the end-bearing capacity of the pile as the area associated with the large shear strain when the settlement was 10% of the pile diameter in the 3D analysis. Yang (2006) obtained the area of influence for the end-bearing capacity of a pile based on the spherical cavity expansion theory (Fig. 9).

Fig. 10 shows the influence area for piles below the pile tip in the 3D analysis. The solid lines indicate the influence

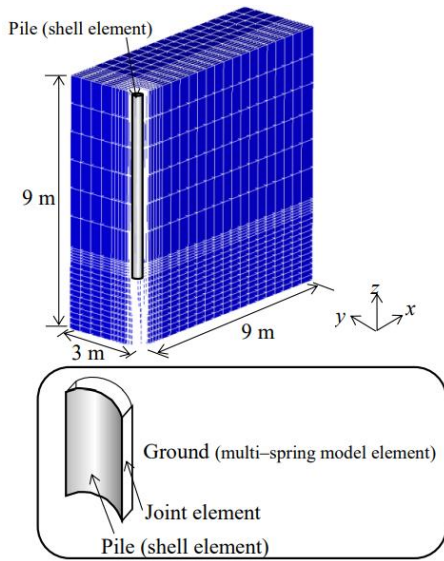


Fig. 6 3D model used in the analysis

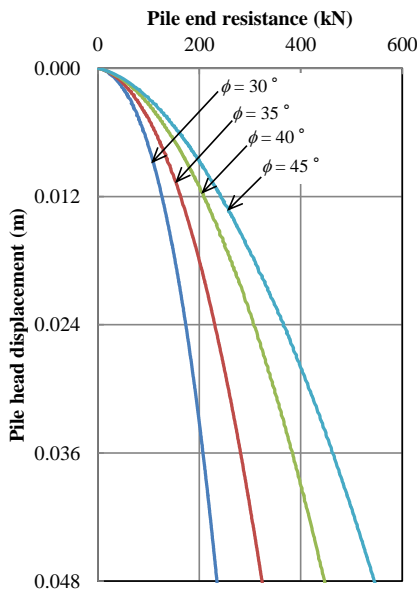


Fig. 7 Relationship between the pile end resistance and pile head displacement (lower layer  $D_r = 90\%$ )

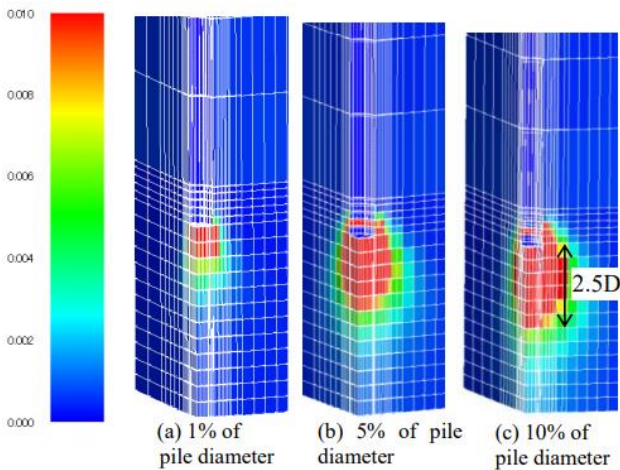


Fig. 8 Maximum shear strain in the 3D analysis ( $D_r = 90\%$ ,  $\phi = 40^\circ$ ) for a settlement of 10% of the pile diameter

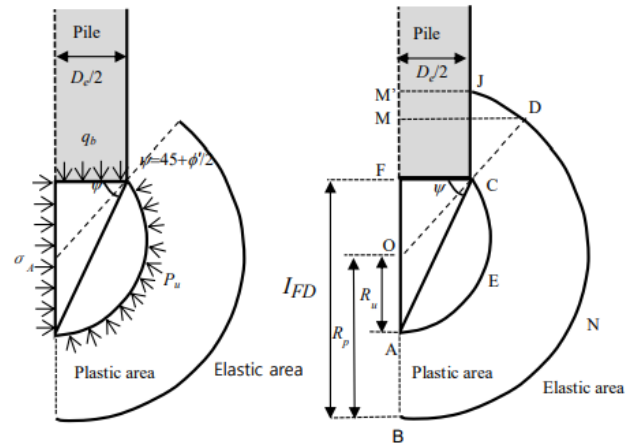


Fig. 9 Influence area for piles below the pile tip (Yang 2006)

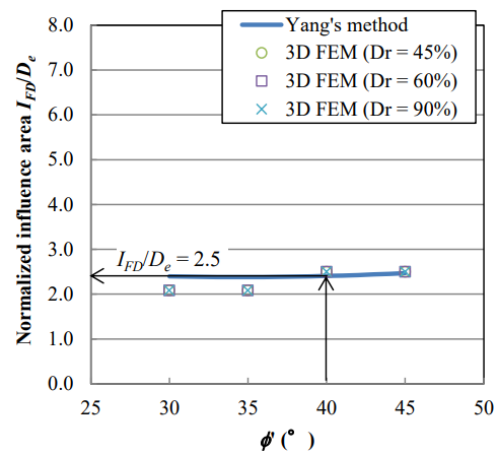


Fig. 10 Influence area for piles below the pile tip for a settlement of 10% of the pile diameter

area for piles below the pile tip proposed by Yang (2006).

The influence area for piles below the pile tip for the end-bearing capacity of a pile in the 3D analysis is approximately the same as that obtained using Yang's method. As shown, the vertical influence area in the 3D analysis is virtually constant. For example, for an internal friction angle of  $40^\circ$ , the ratio of the normalized influence area below the pile tip is 2.5 (i.e.,  $I_{FD}/D_e$ ).

#### 4. Case studies

##### 4.1 Verification with a simple model

We conducted a 2D analysis to examine the characteristics of the proposed Model C. The analysis conditions were the same as those for the model given in Section 2. Fig. 11 shows the 2D mesh used in the analysis. In Model C, the ground nodal points near the pile tip are multi-point constraints, and the constraints of the points have identical deformations. The area of influence was assumed to be 2.5 times the pile diameter based on Fig. 10. The pile penetration was represented as an enforced displacement at the pile head.

Fig. 12 shows the relationship between the pile end

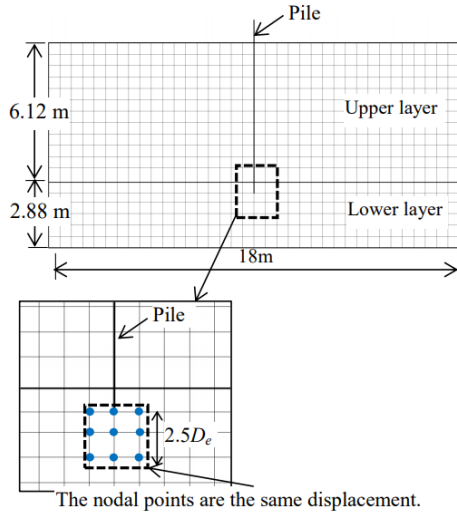


Fig. 11 Two-dimensional mesh model used in the analysis of Model C

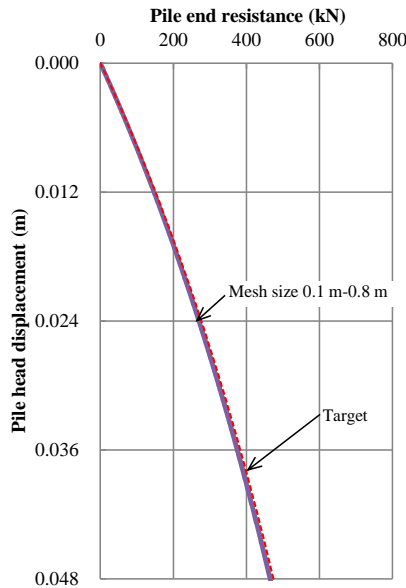


Fig. 12 Relationship between the pile end resistance and the pile head displacement in Model C

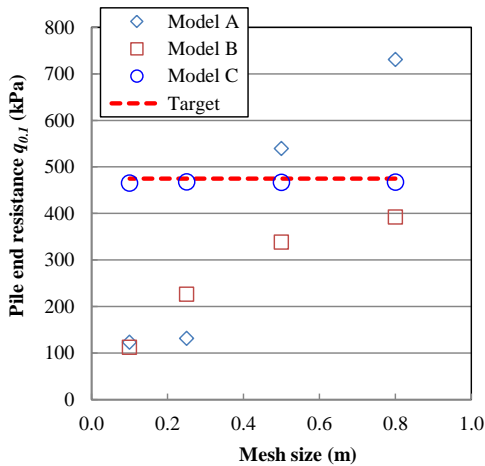


Fig. 13 Relationship between the pile end resistance and the mesh size

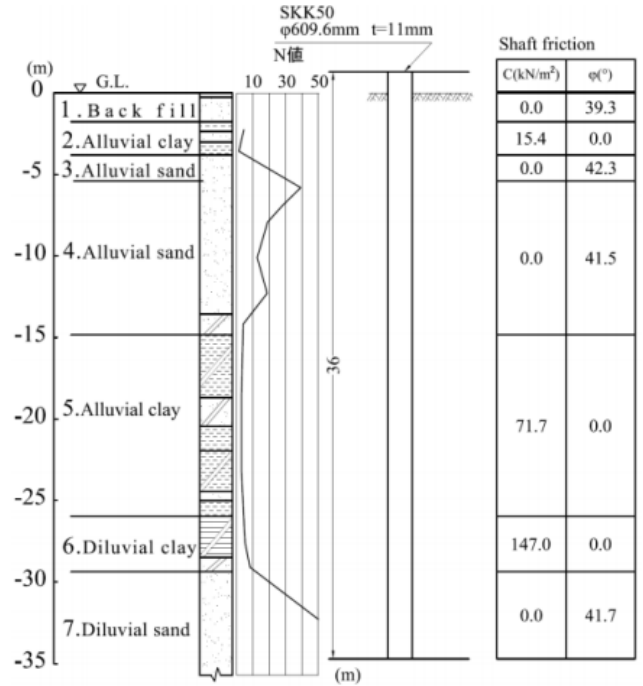


Fig. 14 Soil profile from the loading test

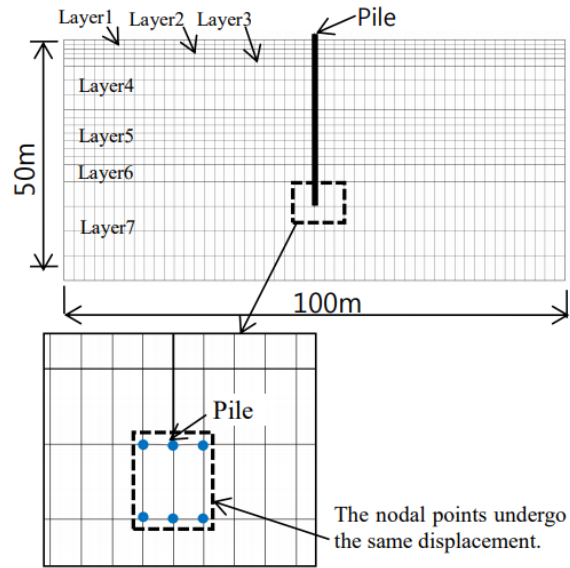


Fig. 15 2D mesh model

resistance and the pile head displacement. As shown in Fig. 4, both the Models A and B fail to reach an agreement with the target. However, the results of Model C are in good agreement with the target, regardless of the mesh size. Fig. 13 shows the summary of the pile end resistance  $q_{0.1}$  at  $0.1D_e$  and the mesh size. Here, the target is based on a hyperbolic approximation. In summary, the pile end behavior can be simulated appropriately in the proposed Model C.

#### 4.2 Verification via an in situ vertical loading test

Tominaga *et al.* (1987) conducted a vertical loading test on a steel pipe pile using the soil profile shown in Fig. 14. The soil parameters used were the same as those listed in

Table 6 Soil parameters

Characteristics	Layer 1	Layer 2	Layer 3	Layer 4	Layer 5	Layer 6	Layer 7
Wet density ( $t/m^3$ )	1.84	1.51	2.02	2.02	1.71	1.71	2.02
Shear modulus $G_{ma}$ (kPa)	$6.63 \times 10^4$	$6.38 \times 10^3$	$1.47 \times 10^5$	$1.25 \times 10^5$	$1.48 \times 10^4$	$5.00 \times 10^4$	$1.32 \times 10^5$
Bulk modulus $K_{ma}$ (kPa)	$1.73 \times 10^5$	$1.66 \times 10^4$	$3.84 \times 10^5$	$3.27 \times 10^5$	$3.85 \times 10^4$	$1.30 \times 10^5$	$3.45 \times 10^5$
Reference confining effective stress $\sigma'_{ma}$ (kPa)	98.0	30.8	98.0	98.0	143.4	182.8	98.0
Reference parameter $m_G, m_K$	0.5	0.5	0.5	0.5	0.5	0.5	0.5
Cohesion $C$ (kPa)	0.0	15.4	0.0	0.0	71.7	147.0	0.0
Internal friction angle $\phi$ ( $^\circ$ )	39.3	0.0	42.3	41.5	0.0	0.0	41.7

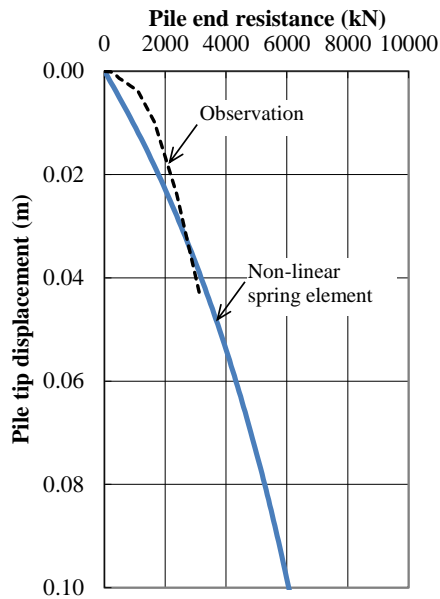


Fig. 16 Properties of the pile tip nonlinear spring element

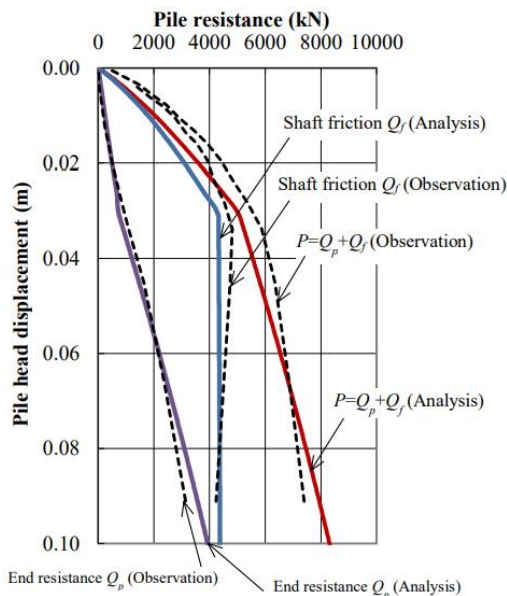


Fig. 17 Relationship between the pile head displacement and the pile resistance in Model C

Table 6, and the 2D mesh was the same as that shown in Fig. 15. For the test, the pile diameter and length ( $L$ ) were

selected as 0.6096 m and 36 m, respectively. The ground comprises seven layers, and fully drained conditions were assumed. All the other conditions were the same as those used in the analysis given in the previous section. The 2D analysis was conducted using a program in the FLIP series (Iai *et al.* 1992). A nonlinear spring element (joint element) was included to simulate the shaft friction along the pile. The shear strength of the nonlinear spring element was made equal to the soil strength. Fig. 14 shows the value of the shaft friction in each layer. Fig. 16 shows the properties of the pile tip nonlinear spring element. The properties were obtained using Eqs. (1) and (5) with the help of the pile end resistance  $q_{0.1}$  at  $0.1D_e$ . The pile end resistance  $q_{0.1}$  is defined by the design values commonly used in Japan (Architectural Institute of Japan 2001) based on the  $N$ -value. This value is consistent with the observed tip resistance in the test. Fig. 17 shows the relationship between the pile resistance and the pile head displacement. The analysis results are in good agreement with the target in terms of the shaft friction  $Q_f$ , end resistance  $Q_p$ , and  $Q_f + Q_p$ . In summary, the pile end behavior is in good agreement with the in situ test results.

## 5. Conclusions

In this paper, we proposed a new pile tip model for the 2D analysis of pile-supported buildings. The following conclusions can be drawn from this study.

(1) We confirmed that the existing pile tip models are problematic. For example, the pile end resistance was found to depend on the mesh size, and the pile end resistance was underestimated, because the ground deformation at the pile tip was counted twice.

(2) To avoid the mesh size effect and to minimize the double counting of the ground deformation, we proposed a new model in which some of the ground nodal points within the area of influence for the end-bearing capacity of a pile were constrained to have the same deformation.

(3) We examined the area of influence below the pile tip based on a 3D analysis. The normalized influence area below the pile tip was found to extend approximately 2.5 times the pile diameter.

(4) We conducted case studies to verify the applicability of the proposed model and found that the pile end resistance was in good agreement with the target.

(5) The proposed model was applied to an in situ vertical loading test. The results showed that the computed

pile resistances (shaft friction  $Q_f$  and end resistance  $Q_p$ ) were in good agreement with the observation.

In the future, the applicability of the proposed model to cases with liquefaction should be examined based on case histories. There has been the trial to obtain the dynamic behaviour of piles via centrifuge (Kim and Choi 2017), and field observations (Chatterjee *et al.* 2015). These types of efforts should be continued.

## Acknowledgements

This research benefitted from discussions in a working group of the FLIP Consortium. The authors sincerely appreciate the contributions and support of the working group members. The authors would like to thank Editage (www.editage.jp) for English language editing, and JSPS Kakenhi for financial support.

## References

- Architectural Institute of Japan. (2001), *Recommendations for Design of Building Foundations* (in Japanese).
- Barr, L. and Wong, R.C.K. (2013) "Shaft resistance of bored cast-in-place concrete piles in oil sand-Case study", *Geomech. Eng.*, **5**(2), 119-142.
- BCP Committee (1971), "Field tests on piles in sand", *Soil. Found.*, **11**(2), 29-49.
- Berezantzev, V.G., Khristoforov, V.S. and Golubkov, V.N. (1961), "Load bearing capacity and deformation of piled foundations", *Proceedings of the 5th International Conference on Soil Mechanics and Foundation Engineering*, Paris, France, July.
- Chatterjee, K., Choudhury, D., Rao, V. and Mukherjee, S.P. (2015), "Dynamic analyses and field observations on piles in Kolkata city", *Geomech. Eng.*, **8**(3), 415-440.
- Fatahi, B., Basack, S., Ryan, P., Zhou, W.H. and Khabbaz, H. (2014) "Performance of laterally loaded piles considering soil and interface parameters", *Geomech. Eng.*, **7**(5), 495-524.
- Hirayama, H. (1988), "A unified base bearing capacity formula for piles", *Soil. Found.*, **28**(3), 91-102.
- Hirayama, H. (1990), "Load-settlement analysis for bored piles using hyperbolic transfer functions", *Soil. Found.*, **30**(1), 55-64.
- Hussien, M.N., Tobita, T., Iai, S. and Rollins, K.M. (2010), "Soil-pile separation effect on the performance of a pile group under static and dynamic lateral loads", *Can. Geotech. J.*, **47**(11), 1234-1246.
- Hyodo, J., Moriyasu, S., Miyashita, K., Uno, K., Ozutsumi, O. and Ichii, K. (2017), "Modeling and parameter determination of pile shaft friction for two-dimensional effective stress analysis", *Ground Eng.*, **35**(1), 27-36 (in Japanese).
- Iai, S. (1993), "Three dimensional formulation and objectivity of a strain space multiple mechanism model for sand", *Soil. Found.*, **33**(1), 192-199.
- Iai, S., Matsunaga, Y. and Kameoka, T. (1992), "Strain space plasticity model for cyclic mobility", *Soil. Found.*, **32**(2), 1-15.
- Kim, Y.S. and Choi, J.I. (2017), "Nonlinear numerical analyses of a pile-soil system under sinusoidal bedrock loadings verifying centrifuge model test results", *Geomech. Eng.*, **12**(2), 239-255.
- Kobayashi, M. (1988), "Stability analysis of geotechnical structures by adaptive finite element procedure", *Rep. Port Harbor Res. Inst.*, **27**(2), 3-22.
- Kumara, J., Kurashina, T., Yajima, T. and Kikuchi, Y. (2015), "Understanding inner friction mechanism of open-ended piles—an experimental study", *Japanese Geotech. Soc. Special Publ.*, **2**(37), 1333-1338.
- Manandhar, S. and Yasufuku, N. (2012), "Analytical model for the end-bearing capacity of tapered piles using cavity expansion theory", *Adv. Civ. Eng.*, 1-9.
- Manandhar, S. and Yasufuku, N. (2013), "Vertical bearing capacity of tapered piles in sands using cavity expansion theory", *Soil. Found.*, **53**(6), 853-867.
- Meyerhof, G.G. (1951), "The ultimate bearing capacity of foundations", *Geotechnique*, **2**(4), 301-332.
- Tamari, Y., Ozutsumi, O., Ichii, K. and Iai, S. (2018), "Simplified method for nonlinear soil-pile interactions in two dimensional effective stress analysis", *Proceedings of the Geotechnical Earthquake Engineering and Soil Dynamics Conference*, Austin, Texas, U.S.A., June.
- Terzaghi, K. (1943), *Theoretical Soil Mechanics*, John Wiley & Sons, New York, U.S.A., 118-136.
- The Overseas Coastal Area Development Institute of Japan (2009), *Technical Standards and Commentaries for Port and Harbor Facilities in Japan*.
- Tominaga, M., Kimura, T., Shiota, K. and Fukaya, T. (1987), "A method for predicting pile behavior based on the in-situ friction meter", *TSUCHI-TO-KISO Japanese Soc. Soil Mech. Found. Eng.*, **35**(12), 43-48 (in Japanese).
- Towhata, I. and Ishihara, K. (1985), "Modelling soil behavior under principal stress axes rotation", *Proceedings of the 5th International Conference on Numerical Methods in Geomechanics*, Nagoya, Japan, April.
- Vesic, A.S. (1972) "Expansion of cavities in infinite soil mass", *J. Soil Mech. Found. Div.*, **98**(SM3), 265-290.
- Wakai, A. and Ugai, K. (1995), "Model tests and analyses on lateral loading behavior of single piles", *J. Geotech. Eng.*, **517**(3-31), 159-168 (in Japanese).
- Wang, Z.J., Xie, X.Y. and Wang, J.C. (2012), "A new nonlinear method for vertical settlement prediction of a single pile and pile groups in layered soils", *Comput. Geotech.*, **45**(9), 118-126.
- Yang, J. (2006), "Influence zone for end bearing of piles in sand", *J. Geotech. Geoenviron. Eng.*, **132**(9), 1229-1237.
- Yasufuku, N. and Hyde, A.F.L. (1995), "Pile end-bearing capacity in crushable sands", *Geotechnique*, **45**(4), 663-676.
- Yasufuku, N., Ochiai, H., and Ohno, S. (2001), "Pile end-bearing capacity of sand related to soil compressibility", *Soil. Found.*, **41**(4), 59-71.
- Zhang, Q.Q., Li, S.C., Liang, F.Y., Yang, M. and Zhang, Q. (2014), "Simplified method for settlement prediction of single pile and pile group using a hyperbolic model", *Int. J. Civ. Eng. Trans. B Geotech. Eng.*, **12**(2), 146-159.
- Zhang, Q.Q., Li, S.C., Liang, F.Y., Yang, M. and Zhang, Q. (2016), "Simplified non-linear approaches for response of a single pile and pile groups considering progressive deformation of pile-soil system", *Soil. Found.*, **56**(3), 473-484.
- Zhang, Q.Q. and Zhang, Z.M. (2012), "A simplified nonlinear approach for single pile settlement analysis", *Can. Geotech. J.*, **49**(11), 1256-1266.